# Density of states of the two-dimensional electron gas studied by magnetocapacitances of biased double-barrier structures

Hou-zhi Zheng, Aimin Song, Fu-hua Yang, and Yue-xia Li
*National Laboratory for Superlattices and Microstructures, Institute of Semiconductors, Academia Sinica, P.O. Box 912, Beijing 100083, China*
(Received 8 June 1993; revised manuscript received 7 September 1993)

The magnetocapacitive response of a double-barrier structure (DBS), biased beyond resonances, has been employed to determine the density of states (DOS) of the two-dimensional electron gas residing in the accumulation layer on the incident side of the DBS. An adequate procedure is developed to compare the model calculation of the magnetocapacitance with the experimental $C$ vs $B$ curves measured at different temperatures and biases. The results show that the fitting is not only self-consistent but also remarkably good even in well-defined quantum Hall regimes. As a result, information about the DOS in strong magnetic fields could reliably be extracted.

## I. INTRODUCTION

While double-barrier structures (DBS) have increasingly attracted great interest for both their potential application in electronic devices and fundamental importance in basic physics, DBS may also serve to probe various physical processes and quantities. For example, magnetotunneling studies in the DBS with a magnetic field $B$ applied perpendicular to the interfaces have provided useful information. On the one hand, the weak oscillations of current or differential conductance observed in the resonance regime makes it possible to deduce the charge build-up in the well and identify the dimensionality of a particular emitter in use.[1–3] On the other hand, the magnetotunneling oscillations, appearing in the off-resonance regime, may be employed to spectroscopically study different nonresonant tunneling processes, either mediated by elastic scattering or assisted by LO phonons.[4,5] Recently, resonant magnetotunneling spectroscopy in an in-plane magnetic field has successfully been used to probe directly the complicated $E(k_{\parallel})$ dispersion relation of hole states in a quantum well.[6]

In the present work we shall demonstrate how the magnetocapacitance of the DBS, biased beyond resonances, can be employed as a reliable method to determine the density of states (DOS) of two-dimensional (2D) electrons residing in the accumulation layer on the incident side of the DBS. Our data convince us that the main advantage of replacing a gated heterostructure by a biased DBS in the determination of the DOS lies in the fact that the accumulation layer in the biased DBS is charged or discharged very fast by exchanging electrons "vertically" with the $n^+$-GaAs electrode in response to an ac modulation signal and no "lateral" magnetoresistance of the 2D channel should be seriously involved. Therefore, the DOS between Landau levels in strong magnetic fields could reliably be extracted from the magnetocapacitance measurements.

In Sec. II we shall derive the theoretical expression of the magnetocapacitance of a DBS, biased beyond resonance regions. The judgment concerning how to identify emitter's dimensionality in a real DBS will be clarified in Sec. III. The model calculation and fitting procedure will be outlined in Sec. IV. Section V contains the main results obtained from the present work and related discussions. Finally we conclude with the summary in Sec. VI.

## II. MAGNETOCAPACITIVE RESPONSE OF A BIASED DBS

To derive the capacitive response, the conduction-band profile of a DBS is schematically depicted in Fig. 1 under the circumstance of interest where the DBS is biased in the voltage range between the first and second resonances. The structural parameters $W_e$, $d_e$, $W$, $d_c$, and $W_c$ indicated in the figure denote the spacer width on the emitter side, the thickness of the emitter barrier, well and collector barrier, and the spacer width on the collector side, respectively. The other letterings have their usual meaning and will become clear later. Since the DBS is biased beyond the resonance regions, charge build-up in

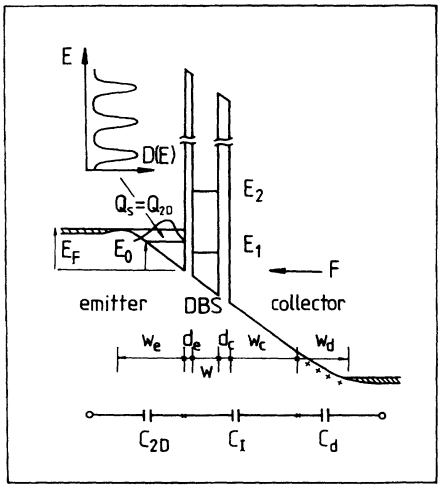


FIG. 1. Conduction-band profile of a positively biased DBS. The inset at the bottom is the lumped circuit of DBS.

 

the central well is negligible and a uniform electric field $F$ will be assumed throughout the regions of $d_e$, $W$, $d_c$, and $W_c$ in the following derivation. The sum rule for the chemical potential difference, $eV$, across the DBS may be expressed as

$$eV = E_F + eW_I F + eV_d \ , \tag{1}$$

where $W_I = W + d_e + d_c + W_c$, the total thickness of the well, two barriers, and the undoped spacer on the collector side. The first term on the right-hand side of Eq. (1) is the Fermi energy on the emitter side, measured from the bottom of the conduction band at the outer interface of the emitter barrier. $eW_I F$ is the potential energy drop across the insulating region. The last term is the potential energy change over the depletion region near the collector electrode, which is approximately evaluated by $\epsilon F^2/2N_d$ with $N_d$ being the doping concentration. We label the total space charge on the emitter side by $Q_S$, which is equal to $Q_S = \epsilon F$, as given by the Gauss theorem. To get the capacitive response of the DBS, one needs to differentiate both sides of Eq. (1) with respect to the applied voltage $V$, and then obtain

$$1 = \frac{C}{C_s} + \frac{C}{C_I} + \frac{Q_S}{e\epsilon N_d} C$$

and

$$1/C = 1/C_S + 1/C_I + 1/C_d \ . \tag{2}$$

Here, $C = dQs/dV$ gives the total capacitance of the DBS. $C_S = edQ_S/dE_F$ is defined as the capacitance of the accumulation layer and $C_d = eN_d\epsilon/Q_S = \epsilon/W_d$ represents the contribution of the depletion layer $W_d$ to the capacitance. $C_I = \epsilon/W_I$ is simply the capacitance of the insulating layer $W_I$. Equation (2) shows that the total capacitance of the DBS is composed of three capacitors in a series in a similar way to that in a gated heterostructure. The capacitance term which concerns us most is

$$C_S = e\frac{d}{dE_F}\int_{E_0}^{\infty} eD(E,E_0,B) f(E,E_F) dE$$

for $T \neq 0$ K and $B \neq 0$T .

For the moment we consider here only the contribution of the 2D electrons to $C_S$. After a straightforward manipulation one is lead to the expression

$$C_S = [1 - dE_0/dE_F] \int_{E_0}^{\infty} e^2 D(E,E_0,B)(-\partial f/\partial E) dE \ . \tag{3a}$$

If a variational calculation for the subband energy $E_0$ is further adopted, Eq. (3a) can explicitly be rewritten as

$$1/C_S = 1 \Big/ \int_{E_0}^{\infty} e^2 D(E,E_0,B)(-\partial f/\partial E) dE + 11\langle z \rangle/32\epsilon \ , \tag{3b}$$

where $D(E,E_0,B)$ is the DOS of the 2D electrons in the presence of magnetic field, $f(E,E_F)$ is the Fermi distribution function, and $\langle z \rangle$ is the standing distance of the 2D electrons in the accumulation layer away from the interface.

Generally speaking, the 3D electrons may coexist with the 2D electrons in the accumulation layer. If their contribution to $C_S$ should be taken into account, then the space charge on the emitter side consists of two parts, $Q_{3D}$ and $Q_{2D}$, as given by $Q_S = Q_{3D} + Q_{2D} = \epsilon F$. Then, $C_S$ will be expressed as

$$C_S = C_{3D} + \int_{E_0}^{\infty} e^2 D(E,E_0,B)(-\partial f/\partial E) dE \times [1 - C_S\langle z \rangle 11/32\epsilon] \tag{4a}$$

and

$$1/C_S = \left\{ \left[ \int_{E_0}^{\infty} e^2 D(E,E_0,B)(-\partial f/\partial E) dE \right]^{-1} + 11\langle z \rangle/32\epsilon \right\} \Big/ (1+\alpha) \ , \tag{4b}$$

where we made use of $edF/dE_F = C_S/\epsilon$. We define

$$\alpha = C_{3D}/C_{2D} \ ,$$
$$C_{3D} = edQ_{3D}/dE_F \ , \tag{5}$$
$$C_{2D} = \int_{E_0}^{\infty} e^2 D(E,E_0,B)(-\partial f/\partial E) dE \ .$$

Apparently, it is desirable to eliminate the contribution of 3D electrons to the capacitance so that the complexity caused by $C_{3D}$ in the determination of the DOS may be avoided, i.e., $\alpha = C_{3D}/C_{2D} = 0$. As verified in some previous work,[3,5,7] it is possible to make all tunneling electrons originate only from 2D electronic states in the accumulation layer by employing a wider spacer or thinner emitter barriers. Then, the determination of the DOS from the magnetocapacitance of a biased DBS becomes simplified in a similar way as to that in a gated heterostructure. Compared with the gated heterostructure, the accumulation layer in the biased DBS will be charged or discharged very fast by exchanging electrons "vertically" with $n^+$-GaAs electrodes and no "lateral" magnetoresistance of the 2D channel should seriously be involved. All the statements asserted here will be testified in the next section.

## III. IDENTIFICATION OF EMITTER'S DIMENSIONALITY

The experiments were done in several AlAs-GaAs-AlAs asymmetrical DBS's, which were similar to those used in Ref. 3. An undoped GaAs well of 75 Å was sandwiched between two undoped AlAs barriers of the thicknesses 25 and 15 Å, respectively. Two undoped GaAs spacers of 200 Å were grown immediately outside the DBS. The full composition of the structures and the fabrication of tunneling diodes were described previously.[3] The general aspects of the measured $I$-$V$ characteristics from the present samples are very similar to the previous one,[5] showing a current peak-to-valley ratio of 20 under forward bias (referring to the top contact being positively biased with respect to the substrate) and a peak-to-valley ratio of 5 in the reverse bias direction. The differential capacitance of the DBS was measured at

two different temperatures, 4.2 and 1.5 K, by a HP 4284A LCR meter with a modulation frequency of 1 MHz and an amplitude of 10 mV as the DBS was biased differently in the voltage region between the first and second resonance peaks. Special attention was paid to the effect of the modulation frequency on the cusplike structures of $C$ vs $B$ curves. One may immediately note that compared with the frequencies ($\sim$20 Hz) used in most previous works,[8] a much higher frequency, 1 MHz was used in this work. However, we found that even in the vicinity of integer fillings no falsely deep minima appeared in the magnetocapacitance, an artifact previously encountered in conventional gated heterostructures due to extremely high magnetoresistance of the 2D channel and, thus, awfully long $RC$ time constant.[9] By further reducing the modulation frequency from 1 MHz to 10 KHz, we carefully checked that no obvious change in either the shapes or the positions of the cusplike dips was found, although the measured results became increasingly noisy. Above observation proved the assertion that charging or discharging the accumulation layer was sufficiently fast to follow the high-frequency modulation signal.

Before using measured $C$ vs $B$ curves for extracting the DOS, it is essential for us to identify the dimensionality of the emitter in a particular DBS. Generally speaking, when the DBS is constructed with two wide undoped GaAs spacers grown directly outside the two barriers, the tunneling processes in the structure can, in principle, be decomposed into two channels. One arises from the resonant tunneling from the 3D states in the emitter (which might spread from the $n^+$-GaAs electrode up to the emitter barrier) to the 2D states in the well (3D-to-2D tunneling). The other is contributed by the resonant tunneling between the 2D states in the accumulation layer and the 2D states in the well (2D-to-2D tunneling). If one is able to judge the existence of pure 2D-to-2D tunneling in one or both bias directions, then the corresponding emitter is only of the 2D electrons, residing in the accumulation layer.

By applying a high magnetic field perpendicular to the interface, we found (see Fig. 2 in Ref. 10) that the reverse $I$-$V$ curve of the device under the investigation was resolved into a doublet peak structure (by the reverse bias we referred to the case where electrons traverse the thicker barrier into the well). One was attributed to the 3D-to-2D tunneling, the other was due to the 2D-to-2D tunneling. However, unlike the reverse $I$-$V$ curve the resonant current peak under forward bias remained single (here forward bias corresponded to the tunneling of electrons into the well trough a thinner barrier). There seemed to be no sign for the presence of the 3D-to-2D tunneling. To be certain, we made a further check. It was well known[3,7,11] that by biasing DBS increasingly in a fixed magnetic field, whenever a discrete Landau level in the well is pulled down below the Fermi energy in the emitter a tunneling channel (denoted by a different Landau index) sets in between a Landau subband in the 3D emitter and a discrete Landau level in the well, leading to a local maximum in the device's conductance. In contrast to the 3D-to-2D tunneling the main resonant peak stemming from the 2D-to-2D tunneling mode should not display any magnetooscillation. This is ascribed to the fact that for a 2D-to2D coherent tunneling the conservation of the energy and the transverse momentum is to restrict the resonance occurring only when two sets of Landau-level ladders (belonging to two different 2D subbands) are exactly in alignment. Therefore, any oscillatory structure which may be revealed on the resonant peak in the $dI/dV$ vs $V$ curve, measured at a particular $B$ field, may serve as a criterion for distinguishing above two tunneling modes. For the forward $dI/dV$ vs $V$ curves measured at different $B$ fields, we found that they were strictly identical to each other with no oscillatory structure discernible (Fig. 2, in Ref. 3). As a consequence, following the above judgment we were convinced that the electrons on the emitter side available for the tunneling in the positive bias direction were of pure two dimensionality for the DBS in use. In other words, the capacitance of the accumulation layer, in this case, only reflects the contribution of 2D electrons, as given by Eq. (3a), so that the determination of the DOS in strong magnetic fields will not be obscured by the possible existence of $C_{3D}$. As a result, in what follows only the $C$ vs $B$ curves of the positively biased DBS will be used for the DOS determination. Figure 2 displays the typical magnetocapacitive

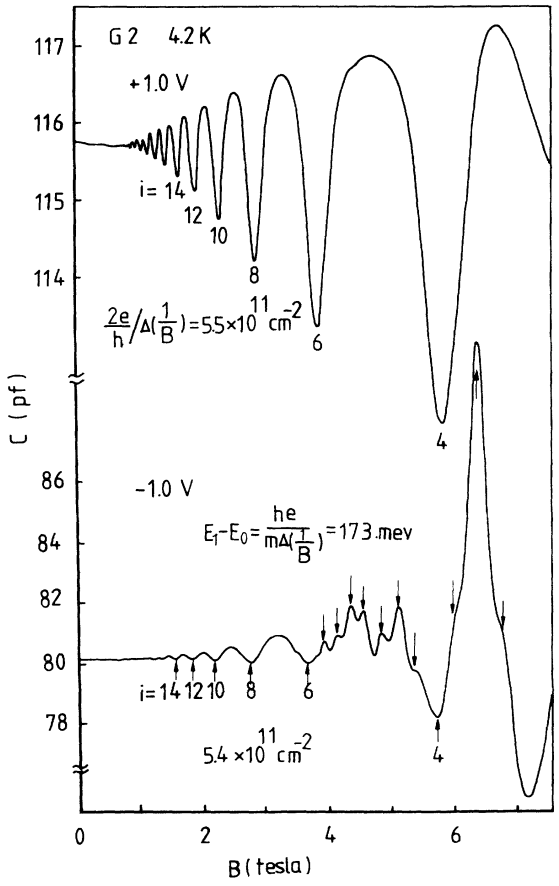


FIG. 2. Magnetocapacitance of DBS, measured at 4.2 K in a sweep of the $B$ field for the biases, $+1.0$ and $-1.0$ V, respectively.

responses of the structure as the DBS is biased in the forward and reverse directions, respectively. The bias voltage is chosen to be about 1.0 V in between the first and second resonant peaks. While the $C$ vs $B$ curve of the positively biased DBS shows clearly cusplike oscillations of relatively larger amplitude, one finds that the corresponding oscillations on the low-field side under the negative bias is obscured and become more sinelike. As for the oscillatory series appearing in the high-$B$ fields it has a different origin, and is attributed to the $\Gamma$-$X$ mixing effect.[12] Above observation can be understood from Eq. (4b). Obviously, taking $C_{3D}$ into account leads to a smearing of the Landau-quantum oscillations, as seen from the lower trace in the figure. Again, this fact is in consistence with our statement that the emitter of the positively biased DBS has a pure 2D nature. Later, our model calculations of $C_S$ will further confirm this point if a nonzero value of $\alpha = C_{3D}/C_{2D}$ is assumed [see Eq. (5)].

## IV. MODEL CALCULATION AND FITTING

In what follows, we shall perform a model calculation of the magnetocapacitance in a DBS with a Gaussian-like DOS of the form

$$D_G(E)=\frac{eB}{2h}\sum_n\left[\frac{2}{\pi}\right]^{1/2}\frac{1}{\Gamma_n}\left\{e^{-(E-E_{n\uparrow})^2/2\Gamma_n^2}+e^{-(E-E_{n\downarrow})^2/2\Gamma_n^2}\right\}. \quad (6)$$

Here

$$E_{n\uparrow,\downarrow}=E_0+(n+1/2)\hbar\omega_c \mp g^*\mu_B B/2 \quad (7)$$

are the spin-resolved Landau levels. The enhancement of spin splitting due to interaction effect is taken into account in the usual way:

$$g^*=g_0+(E_{ex}/\mu_B B)(N_{2D\uparrow}-N_{2D\downarrow}) \quad (8)$$

and

$$N_{2D\uparrow,\downarrow}=\int_{E_0}^{\infty}dE\, f(E,E_F)\frac{eB}{2h}\times\sum_n\left[\frac{2}{\pi}\right]^{1/2}\frac{1}{\Gamma_n}e^{-(E-E_{n\uparrow,\downarrow})^2/2\Gamma_n^2} \quad (9)$$

$$N_{2D}=N_{2D\uparrow}+N_{2D\downarrow}\ , \quad (10)$$

where $g_0=0.52$ is the Lande factor in the absence of the many-body effect, $E_{ex}$ is the interaction coefficient and taken as a fitting parameter, and $N_{2D\uparrow}$ and $N_{2D\downarrow}$ give the number density of the 2D electrons filled in the spin-up and spin-down states, respectively. The broadening parameter used in Eqs. (6) and (9) $\Gamma_n$ is assumed to be of the dependence of $\Gamma=\Gamma_0 B^{1/2}$. Quite often, in order to fit the data one has to introduce a constant background in the model DOS, as given by

$$D_{GB}(E)=D_G(E)(1-x)+xm^*/\pi\hbar^2\ . \quad (11)$$

The employed fitting procedure is summarized as follows.

(1) At a given 2D number density $N_{2D}$ self-consistently solve the Schrödinger equation and Poisson equation, and consequently obtain the numerical dependence of the ground subband energy on the 2D number density, $E_0(N_{2D})$.

(2) Since the doping concentration of the $n^+$-GaAs layer $N_d$ is usually not a quantity which may accurately be known from material growth, we shall determine it in the following way. We first use the magneto-oscillations observed on the $C$ vs $B$ traces to get $N_{2D}$ from their periods in the reciprocal of $B$ fields $\Delta(1/B)$ and obtain the experimentally derived relation $N_{2D}(V)$ or its inverse relation $V(N_{2D})$. Next, we make use of Eq. (1) and rewrite it approximately in the form of

$$V\approx\frac{\pi\hbar^2}{m^*}N_{2D}+E_0(N_{2D})+\frac{eN_{2D}}{\epsilon}W_I+\frac{eN_{2D}^2}{2\epsilon N_d}\ , \quad (12)$$

where the first term on the right-hand side $\pi\hbar^2 N_{2D}/m^*$ is approximately equal to $E_F-E_0$, $E_0(N_{2D})$ is taken from the calculation made in step (1), $W_I=d_e+W+d_c+W_c=315$ Å, as given by the structural parameters. Finally, we fit Eq. (12) to the measured relation $V(N_{2D})$ so that the doping concentration $N_d$ can be determined. For the DBS in use, $N_d$ takes a value of $3.5\times10^{16}$ cm$^{-3}$. Figure 3 shows such a fitting, where the dots are the experimental points and the solid line is the fitting curve from Eq. (12).

(3) Take $E_F-E_0$, $g^*$, $E_0$, $N_{2D\uparrow}$, and $N_{2D\downarrow}$ as unknown variables, and self-consistently solve Eqs. (7)–(10) and the following equation:

$$E_F-E_0=V-E_0(N_{2D})-\frac{eN_{2D}}{\epsilon}W_I-\frac{eN_{2D}^2}{2\epsilon N_d}$$

[from Eq. (1)], (13)

where the relation $E_0(N_{2D})$ is again taken from step (1).

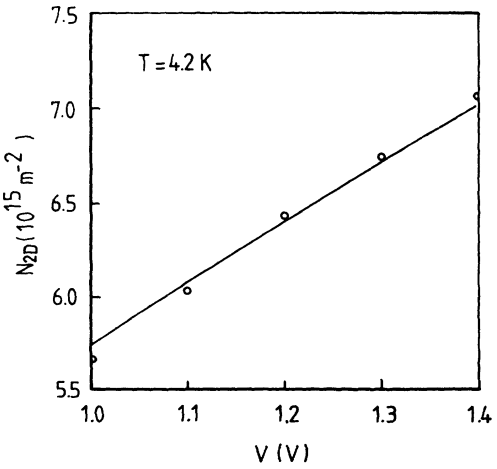


FIG. 3. Depenences of $N_{2D}$ on the bias V. Dots are the measured points; the solid line is the fitting from Eq. (12) with $N=3.5\times10^{16}$ cm$^{-3}$.

As a result, the dependencies on the $B$ field of $E_F - E_0$, $g^*$, $E_0$, $N_{2D\uparrow}$, $N_{2D\downarrow}$, and $D(E)$ can finally be calculated.

(4) Substitute them into Eqs. (2) and (3) to get the calculated $C$ vs $B$ curve, and compare it with the measured one.

(5) Adjust the fitting parameters $\Gamma_0$, $E_{ex}$, and $x$ and iterate steps (3) and (4) until a satisfactory fitting is finally achieved for different bias voltages and temperatures.

## V. RESULTS AND DISCUSSIONS

The fitting procedure outlined in Sec. III has been completed for two different temperatures 4.2 and 1.5 K and two different biases 1.1 and 1.3 V, as shown in Figs. 4 and 5, respectively. From these figures it is convincing to conclude that the model fitting completed in the present work is not only self-consistent with a unique set of the parameters: $\Gamma_0 = 0.56$ meV$/\sqrt{T}$, $E_{ex} = 3.143 \times 10^{-11}$ meV cm$^2$, and $x = 28\%$ ($W_I = 315$ Å, $N_d = 3.5 \times 10^{16}$ cm$^{-3}$) used for different biases and temperatures, but also remarkably good over a wide field range up to 7T, especially in the vicinity of integer fillings, where such a comparison was previously considered as an inappropriate practice in conventional gated heterostructures. The fitting parameters used here does not necessarily mean the optimized choice, and one may improve the fitting further. However, by a close look of the figures one may find that in certain range (not a whole range) of the $B$ fields some small discrepancies were just discernible at the capacitance maxima and minima. This is presumably attributed to the fact that a tiny amount of electron charge may accumulate in the central well at the biases higher than 1.0 V. A similar Landau quantum oscillation will emerge but with a much longer period in $1/B$. This will give rise to a weak modulation on both the amplitude and the dip position of the main oscillatory series. This is roughly what we have found in the figures.

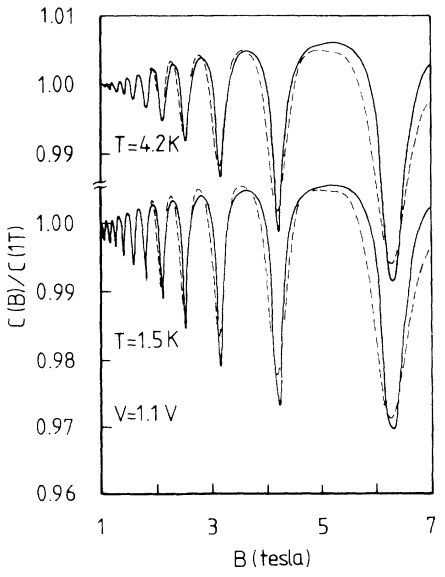


FIG. 4. Magnetocapacitance curves at 4.2 and 1.5 K, normalized by its value at $B = 1$ T, as DBS is biased at $+1.1$ V. Dashed line is from the measurements. Solid curve is the model fitting.

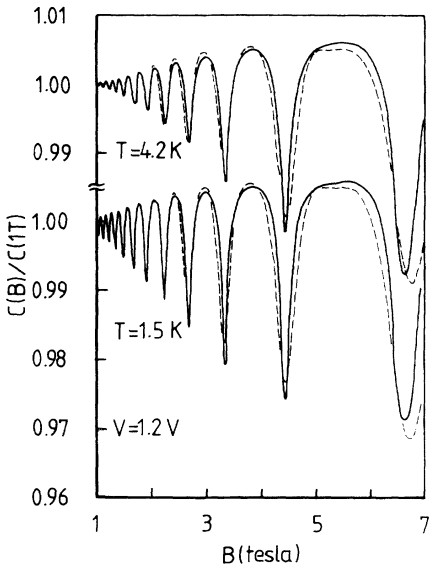


FIG. 5. Magnetocapacitance curves at 4.2 and 1.5 K, normalized by its value at $B = 1$ T, as DBS is biased at $+1.3$ V. Dashed line is from the measurements. The solid curve is the model fitting.

In order to check the effect of $C_{3D}$, we take one step further. By using Eq. (4), we have also tried to include the contribution of 3D mobile electrons in the magnetocapacitance to see if they should play some role. For simplicity, we set $\alpha$, the ratio of $C_{3D}$ to $C_{2D}$, be a constant of 0.2. What we found is a noticeable decrease in both maxima and minima of the oscillations in the calculated magnetocapacitance. The fitting becomes worse. To some extent, the above trial justifies our previous statement that under the forward bias only the 2D electrons in the accumulation layer make a contribution to the structural capacitance.

The model DOS in strong magnetic fields, obtained from the fittings performed at the biases 1.1, 1.2, and 1.3 V, are plotted in Fig. 6 as the $B$ field is fixed at 7 T. The

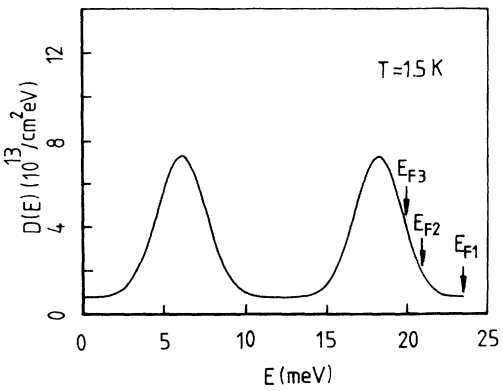


FIG. 6. Model DOS from the fittings performed in Figs. 4 and 5, as $B = 7$ T. $E_{F1}$, $E_{F2}$, and $E_{F3}$ are the Fermi energies for the biases 1.3, 1.2, and 1.1 V, respectively.

overall features of the DOS are similar to that in the previous study,[8,13] but over a much wider $B$ field range (up to 7 T). Especially in the quantum Hall regimes, reliable information about the DOS has been extracted from the magnetocapacitance. The DOS shows a nonvanishing value about 28% of the DOS in the zero field between Landau levels. A nonvanishing DOS between Landau levels may originate from inhomogeneities in the structure, e.g., the fluctuation in the 2D number density in the plane.[12] On the other hand, the effective width of Landau levels may change in an oscillatory way as they lift up successively across $E_F$ with the $B$ field. A maximum level broadening is expected to occur at the integer fillings, where small DOS makes the screening to ionized impurities less effective.[14] If this is true, what we have extracted is some sort of the averaged DOS. Our data also seem to confirm the $\sqrt{B}$ dependence of the level broadening over a wide $B$ field range from 1 to 7 T, as predicted by the self-consistent Born approximation.[15]

In a biased DBS, the chemical potential difference across the structure pins at the value of $eV$ as given by Eq. (1). This makes the situation different from that in an ungated structure. Strictly speaking, in order to maintain self-consistency the subband energy $E_0$ and the 2D number density $N_{2D}$ cannot remain constant as the magnetic field sweeps up and down. From our self-consistent calculation it follows that the physical quantities obtained from the fitting, such as $E_0$, $N_{2D}$, Fermi energy $E_F-E_0$, and effective Lande factor $g^*$, all show oscillatory change with the $B$ field. The bottom trace in Fig. 7 gives the variation of $D(E_F)$, the DOS at the Fermi level, as a function of the $B$ field at 1.5 K and $V=1.2$ V. The top two traces are plotted for the relations of $E_0$ vs $B$ and $N_{2D}$ vs $B$, extracted from the fitting at the same conditions. One finds that both $E_0$ and $N_{2D}$ have a rapid jumping as $E_F$ crosses the integer filling, leading to a very small transient current through the DBS.[13] Nevertheless, the variations in $E_0$ and $N_{2D}$ are very small and no larger than $6\times10^{-4}$ and $1\times10^{-3}$, respectively. The top two traces in Fig. 8 display the oscillation changes for the $E_F-E_0$ and $g^*$ factor in a sweep of $B$ fields. The $D(E_F)$ vs $B$ trace is again plotted at the bottom as a reference. Even in the present case where the spin-split peak is not clearly seen, the effective Lande factor $g^*$ oscillates, showing a large enhancement and reaching a maximum of about 3.6 at 5.4 T.

Finally, we point out that prior to present work there have been several techniques proposed to eliminate the in-plane resistance of the 2D conducting channel in the measurement of $C$ vs $B$ curves by means of vertically charging two-dimensional electron gas (2DEG). Hickmott[16] and Eaves[17] measured the $I$-$V$, $dI/dV$-$V$, and $C$-$V$ characteristics at fixed magnetic fields in $n^-$-GaAs/$Al_xGa_{1-x}As$/$n^+$-GaAs and $n^-$-(InGa)As/InP/$n^+$ (InGa)/As single-barrier structures, respectively. They observed the oscillatory structures of Shubnikov de-Hass type due to magnetotunneling through a single barrier from the 2DEG in the emitter accumulation layer. No adequate theoretical model and fitting procedure were developed to extract the DOS information from the capacitance data. Smith III[18] employed GaAs/$Al_xGa_{1-x}As$ heterostructure capacitors, and measured the DOS in the presence of magnetic field for the 2DEG adjacent to a single, thick nonconducting $Al_xGa_{1-x}As$ barrier. In contrast to previous experiments, where the conductivity in the plane of the 2DEG limited DOS measurements to lower magnetic fields,[19] in above these works they were able to extend the measurements into higher magnetic fields, even the fractional

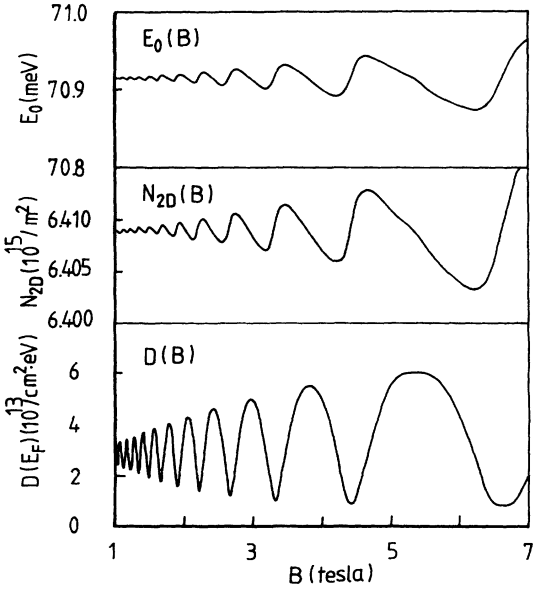


FIG. 7. Dependences on $B$ fields of $E_0$, $N_{2D}$, and $D(E_F)$, obtained self-consistently from the model fitting at $T=1.5$ K and $V=1.2$ V.

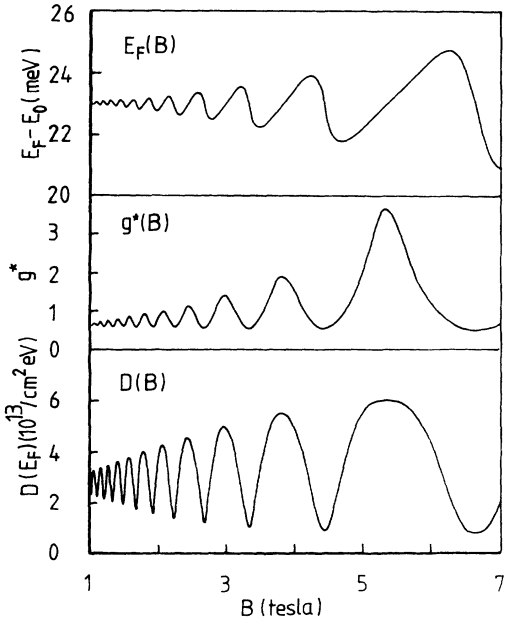


FIG. 8. Dependences on $B$ fields of $E_F-E_0$, $g^*$, and $D(E_F)$, obtained self-consistently from the model fitting at $T=1.5$ K and $V=1.2$ V.

Hall regime, by allowing electrons to flow in and out of the 2DEG from a heavily doped electrode. However, no clear evidence was provided that one can exclude the possible contribution to the structural capacitance of 3D electrons, which might quite often coexist with the 2DEG in the accumulation layer. The use of a biased DBS in the DOS measurements, as verified in present work, has two folds. On one hand, the existence of 3D electrons with 2D electrons on the incident side of a DBS is a common phenomenon, as proved by two different modes of resonant tunneling—3D-to-2D tunneling and 2D-to-2D tunneling. The ignorance of the above fact in both DBS as well as single-barrier structure may lead to incorrect information for the DOS [as shown by Eq. (4)]. On the other hand, as demonstrated in the Sec. III, the different characteristic features of two modes in resonant magnetotunneling justify their use in judging the only presence of 2D electrons in the accumulation layer adjacent to the incident barrier. One may suggest that by tilting the magnetic field away from the normal of samples one is able to examine the 2D nature of the electrons in the emitter accumulation layer.[20] However, that is not quite true. One can only prove the "existence" of the 2DEG in that way, but cannot rule out the possible simultaneous presence of 3D electrons. The reason for this is simple. The cusplike dips revealed in $C$ vs $B$ traces reflect mainly the oscillatory change in the DOS of 2D electrons near the Fermi level, which usually prevails over the effect from the 3D electrons. Thus, seeing the quantum oscillations does not mean that one can definitely exclude the possible presence of 3D electrons. The contribution of 3D electrons is to smear the quantum oscillation in a manner as described by Eq. (4) and shown by the lower trace in the Fig. 2. In this regard, therefore, the use of a biased DBS is of essential importance in the DOS determination, as compared with single-barrier structures. Ashoori and Sisbee[21] employed a tunneling barrier to realize the vertical charge transfer between an $n^+$-GaAs emitter and an undoped GaAs quantum well (where the 2DEG resided), and obtained the Landau DOS up to a magnetic field of 4 T. Presumably limited by still relatively high tunneling resistance, no information of the DOS in the well-defined quantum Hall regime was shown.

## VI. SUMMARY

We have derived the theoretical expression of the magnetocapacitance of a biased DBS, and developed an adequate procedure to fit the model calculation with the experimential $C$ vs $B$ curves measured at different temperatures and biases. It turns out that the fitting, performed in present work, is not only self-consistent but also remarkably good over a wide $B$-field range up to 7 T. Our results justify the statement that replacing a gated heterostructure by a biased DBS enables one to extract the reliable information about the DOS from the magnetocapacitance, especially in the quantum Hall regime.

## ACKNOWLEDGMENTS

We would like to thank the technical assistance of C. F. Li. The work at the National Laboratory for Superlattices and Microstructures, Institute of Semiconductors, Academia Sinica is supported by the State Council of Science and Technology.

[1]A. Zaslavsky, D. C. Tsui, M. Santos, and M. Shayegan, Phys. Rev. B **40**, 9829 (1989).

[2]M. L. Leadbeater, E. S. Alves, F. W. Sheard, L. Eaves, M. Henini, O. H. Hughes, and G. A. Toombs, J. Phys. Condens. Matter **1**, 10 605 (1989).

[3]H. Z. Zheng and F. H. Yang, in *Proceedings of International Conference on Semiconductor Physics,* edited by E. M. Anastassakis and J. D. Joannspoulos (World Scientific, Singapore, 1990), p. 1317.

[4]M. L. Leadbeater, E. S. Alves, L. Eaves, M. Henini, O. H. Hughes, A. Celeste, J. C. Portal, G. Hill, and M. A. Pata, Phys. Rev. B **39**, 3438 (1989).

[5]H. Z. Zheng, F. H. Yang, and Z. G. Chen, Phys. Rev. B **42**, 5270 (1990).

[6]R. K. Hayden, D. K. Maude, L. Eaves, E. C. Valadares, M. Henini, F. W. Sheard, O. H. Hughes, J. C. Portal, and L. Cury, Phys. Rev. Lett. **66**, 1749 (1991).

[7]V. J. Goldman and B. Su, in *Resonant Tunneling in Semiconductors: Physics and Applications,* Vol. 277 of *NATO Advanced Study Institute Series B: Physics* edited by L. L. Chang, E. E. Mendez, and E. Tejedor (Plenum, New York, 1991), p. 431.

[8]T. P. Smith, B. B. Goldberg, P. J. Stiles, and M. Heiblum, Phys. Rev. B **32**, 2696 (1985).

[9]R. K. Goudall, R. J. Higgins, and P. J. Harrang, Phys. Rev. B **31**, 6597 (1985).

[10]H. Z. Zheng and F. H. Yang, in *Resonant Tunneling in Semiconductors: Physics and Applications* (Ref. 7), p. 175.

[11]E. E. Mendez, L. Esaki, and W. I. Wang, Phys. Rev. B **33**, 2893 (1986).

[12]H. Z. Zheng, F. H. Yang, J. Liu, Y. X. Li, and A. M. Song, Superlatt. Microstruct. **12**, 279 (1993).

[13]V. Mosser, D. Weiss, K. v. Klitzing, K. Ploog, and G. Weimann, Solid State Commun. **58**, 5 (1986).

[14]W. Cai and T. S. Ting, Phys. Rev. B **33**, 3967 (1986).

[15]T. Ando, Y. Vemura, J. Phys. Soc. Jap. **6**, 959 (1974).

[16]T. Hickmott, Phys. Rev. B **32**, 6531 (1985).

[17]L. Eaves, B. R. Snell, D. K. Maude, P. S. S. Guimaraes, D. C. Taylor, F. W. Sheard, G. A. Toombs, J. C. Portal, L. Dnowski, P. Claxton, G. Hill, M. A. Pate, and S. J. Bass, *Proceedings of the International Conference on Physics of Semiconductors,* edited by O. Engström (World Scientific, Singapore, 1986), p. 1615.

[18]T. P. Smith III and W. I. Wang, Phys. Rev. B **34**, 2995 (1986).

[19]R. K. Goudall, R. J. Higgins, and P. J. Harrang, Phys. Rev. B **31**, 6597 (1985).

[20]M. L. Leadbeater, E. S. Alves, F. W. Sheard, L. Eaves, M. Henini, O. H. Hughes, and G. A. Toombs, J. Phys. Condens. Matter **1**, 10 605 (1989).

[21]R. C. Ashoori and R. H. Silsbee, Solid State Commun. **81**, 821 (1992).